CHEMBIOCHEM

DOI: 10.1002/cbic.200700767

An Amphiphilic Bisporphyrin and Its Yb^{III} Complex: Development of a Bifunctional Photodynamic Therapeutic and Near-Infrared Tumor-Imaging Agent

Feng-Lei Jiang,[a, b] Chun-Ting Poon,[b] Wai-Kwok Wong,*[b, c] Ho-Kee Koon,[d] Nai-Ki Mak,*[d] Chun Yu Choi,[b] Daniel W. J. Kwong,*[b] and Yi Liu*[a]

Cancer is one of the leading causes of death worldwide. Photodynamic therapy (PDT) is an emerging inherently selective cancer-treatment modality under active investigation by both clinicians and basic scientists.[1] In PDT, the activation of a nontoxic photosensitizer by light of an appropriate wavelength (energy) enables it to transfer some of its excitation energy to molecular oxygen. Reactive oxygen species thus generated, such as singlet oxygen ($^1O_2$), in turn cause oxidative stress and damage to the target tissues, which results in cell death.

Porphyrin-based photosensitizers have been studied extensively during the past two decades. Porphyrin derivatives were found to accumulate readily in tumors, presumably because of their high vascular permeability, as well as their affinity for proliferating endothelium, and the lack of lymphatic drainage in tumors.[2] However, the mechanism by which porphyrins accumulate selectively in tumors is still not fully understood. In general, porphyrin derivatives, which absorb strongly in the visible region, are efficient singlet-oxygen generators. One cationic porphyrin, namely, meso-tetrakis(*N*-methylpyridinium-4-yl)porphyrin (H_2TMPyP), has been investigated extensively owing to its water solubility and biocompatibility. However, these studies have focused mainly on its in vitro interactions with DNA.[3] The more clinically relevant studies of its photodynamic activity towards tumor cells are less well-documented, presumably as a result of the fact that H_2TMPyP is too hydrophilic to pass through the lipophilic cell membranes. To overcome this problem, attempts were made to increase its cellular uptake by conjugation with poly-(*S*)-lysine and amphipathic peptides.[4]

Another frontier development involves the design of bifunctional PDT agents with the ability to both photosensitize and image tumor cells.[5] For example, the photosensitizer pyropheophorbide a conjugated with Gd^{III}–DTPA (DTPA = diethylenetriaminepentaacetic acid), which serves as a magnetic resonance imaging (MRI) contrasting agent, was used in a "see and treat" approach, whereby drug uptake by the tumor was monitored by MRI techniques and then followed by targeted photodynamic treatment.[5a] Other examples include Gd^{III}–texaphyrin. Texaphyrin is a water-soluble tripyrrolic pentaaza-expanded porphyrin capable of coordinating the large lanthanide cation. In this case, the Gd^{III} complex acts as an X-ray computed tomography (CT) enhancing agent as well as a PDT agent.[5d] These bifunctional PDT agents, although novel and efficacious, involve the use of rather costly imaging technologies, that is, MRI, CT, positron emission tomography (PET), and single photon emission computed tomography (SPECT). Near-infrared (NIR) fluorescence (650–900 nm) imaging with indocyanine dyes, which can be conjugated with various target-specific low-molecular-weight ligands, offers a highly promising and less costly alternative.[6] NIR imaging has a number of advantages: 1) As NIR light is not absorbed by tissues and body fluids, deep-tissue imaging is possible; 2) highly sensitive detectors (for example, InGaAs) and data-processing techniques are available for quantitative and real-time NIR imaging; 3) imaging in this region minimizes tissue autofluorescence and therefore leads to a substantial enhancement of target/background ratios.[7] In fact, endoscopic NIR imaging with a fiber-optic sensor was demonstrated recently.[8] Inorganic NIR emitters, such as Yb^{III}–porphyrinate complexes, have also been described for tumor imaging.[9] Although lower quantum yields are observed for the lanthanide(III) NIR emitters (for example, Yb^{3+} and Nd^{3+}) than for the indocyanine dyes, the lanthanide(III) NIR emitters have received considerable recent attention because of their longer (microsecond-range) luminescence lifetimes, which allow for more signal accumulation, and their longer NIR-emission wavelengths (> 1000 nm), which further improve the target/background ratios.[10]

In this study, we improved the cellular uptake of cationic porphyrin by increasing its hydrophobicity through the synthesis of an amphiphilic bisporphyrin, **1**. Furthermore, we prepared a Yb^{III}–bisporphyrin complex, Yb·**1**, which emitted strongly in the NIR region (at ca. 1000 nm) upon its uptake by cells and exhibited substantial PDT activity towards the rat tumor-cell model Sarcoma 180. These results, together with

[a] *F.-L. Jiang, Y. Liu*
College of Chemistry and Molecular Sciences, Wuhan University
Wuhan 430072 (P. R. China)
Fax: (+86) 27-68754067
E-mail: prof.liuyi@263.net

[b] *F.-L. Jiang, C.-T. Poon, W.-K. Wong, C. Y. Choi, D. W. J. Kwong*
Department of Chemistry, Hong Kong Baptist University
Kowloon Tong, Hong Kong (P. R. China)
Fax: (+852) 3411-7348
E-mail: wkwong@hkbu.edu.hk
dkwong@hkbu.edu.hk

[c] *W.-K. Wong*
Centre for Advanced Luminescence Materials, Hong Kong Baptist University
Kowloon Tong, Hong Kong (P. R. China)

[d] *H.-K. Koon, N.-K. Mak*
Department of Biology, Hong Kong Baptist University
Kowloon Tong, Hong Kong (P. R. China)
Fax: (+852) 3411-5995
E-mail: nkmak@hkbu.edu.hk

Supporting information for this article is available on the WWW under http://www.chembiochem.org or from the author.

the DNA-photocleavage and $^1O_2$-generating activity of Yb·**1**, suggest that this complex may serve as a novel "see and treat" bifunctional PDT agent.

The bisporphyrins **1** and Yb·**1** (Scheme 1; see Scheme S1 in the Supporting Information for their preparation) were characterized by high-resolution mass spectrometry (HRMS) and

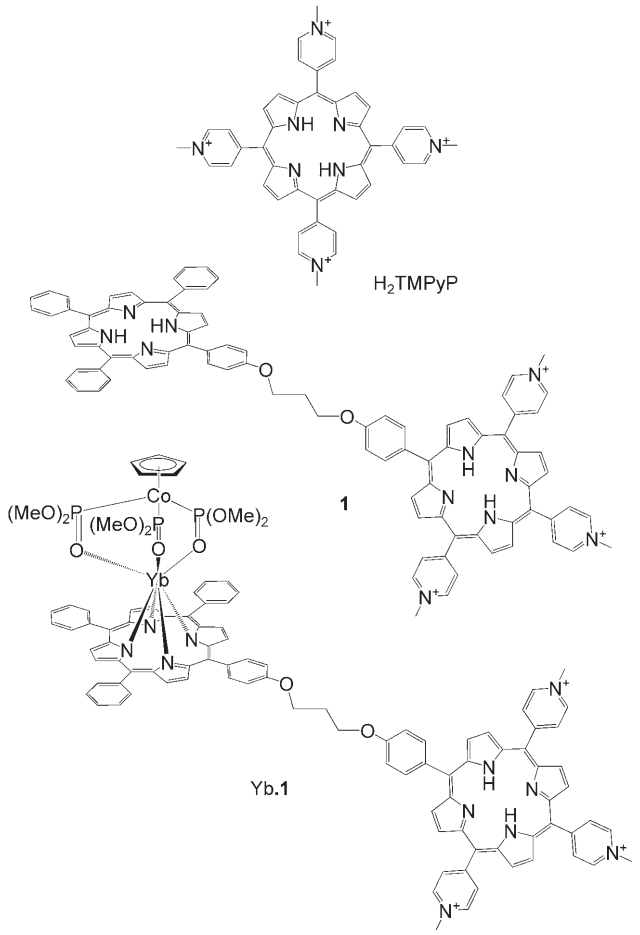

Scheme 1. Structures of H_2TMPyP and the bisporphyrins **1** and Yb·**1** with chloride ions (not shown) as the counter ions.

^{1}H NMR, ^{31}P NMR (for Yb·**1**), UV/Vis, and fluorescence spectroscopy. The absorption spectra of **1** and Yb·**1** (Figure S1) show absorption maxima at 422 and 427 nm, respectively, and their steady-state fluorescence spectra (Figure S2) show the same red-emission peak at 661 nm in water.

In Yb·**1**, the Yb^{III} ion is coordinated to the porphyrin macrocycle, which upon photoirradiation transfers the triplet-excited-state energy to the metal. The metal in turn loses this energy radiatively as NIR emission.[11] This intramolecular energy transfer, whereby the hydrophilic TMPyP moiety acts as an antenna for light absorption and Yb^{III} as the NIR emitter, is described in Figure 1 for the irradiation of Yb·**1** at 514 nm, a wavelength sufficiently close to the region in which only TMPyP is photoexcited. Emission at 1000 nm was observed.[12] An anionic tripodal ligand, L_{OMe}^- ((cyclopentadienyl)tris(dimethylphosphito)-cobaltate), was used to encapsulate the Yb^{III} ion to 1) ensure

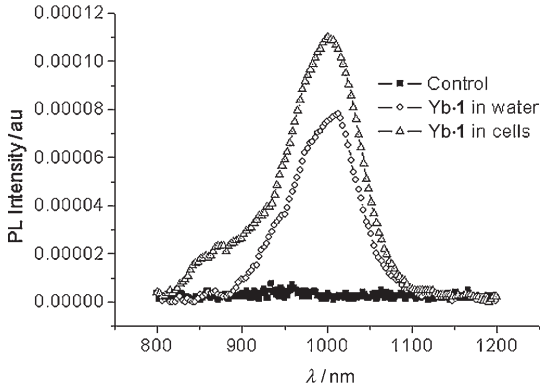

Figure 1. Photoluminescence (PL) spectra of a control, Yb·**1** in water, and a suspension of Sarcoma 180 cells loaded with Yb·**1** upon excitation with argon-ion-laser light at 514 nm. The cell suspension loaded with Yb·**1** was prepared as follows: Sarcoma 180 cells were incubated with Yb·**1** for 22 h, then centrifuged, washed thoroughly, and resuspended in phosphate-buffered saline (PBS). The control sample consisted of Sarcoma 180 cells that had not been treated with Yb·**1**.

the integrity of the complex and 2) prevent deactivation and/or quenching of its NIR fluorescence by solvent molecules under physiological conditions.[13] The NIR-luminescence lifetime of Yb·**1** in water is 10.13 ± 0.05 μs (Figure S3). As the NIR-luminescence lifetimes observed for most lanthanide(III) complexes in aqueous media[10] lie in the microsecond range, this result confirmed the structural integrity of Yb·**1**. It is vitally important that the NIR-luminescence lifetime lies within this range if a Yb^{III} complex is to act as an NIR-luminescent probe. The NIR-emission spectrum of Yb·**1** in an aqueous environment is similar to the emission spectrum of Yb·**1** in a cell suspension recovered after incubation with Yb·**1** and thorough washing (Figure 1).

The relative $^1O_2$ yields of H_2TMPyP, **1**, and Yb·**1** were determined by using 1,3-diphenylisobenzofuran (DPBF) as an $^1O_2$-selective chemical trap. The reaction of DPBF with $^1O_2$ produces a product that does not absorb light at wavelengths above 400 nm.[14] The absorbance of DPBF at 415 nm decreased with increasing photoirradiation time of the porphyrins (Figure 2). The following relative rates of $^1O_2$ production by these porphyrins were derived from the steepness of the slopes of the curves in Figure 2: H_2TMPyP (20.5) > **1** (4.1) > Yb·**1** (1.0). The fourfold lower $^1O_2$-production rate of Yb·**1** relative to that of **1** is presumably due to the channeling of a substantial fraction of its photoexcitation energy to the Yb^{III} center, which then emits the energy in the NIR region. The reason for the substantially lower $^1O_2$-production rate of **1** relative to that of H_2TMPyP is not clear at present.

As $^1O_2$ can cause DNA scission, the DNA-photocleavage activities of **1** and Yb·**1** were examined by gel electrophoresis by using a plasmid-DNA-relaxation assay. We found that both bisporphyrins can cleave DNA in a concentration-dependent manner upon photoirradiation (Figures S4 A and S4 B). Furthermore, their DNA-photocleavage activities are similar, despite the distinct $^1O_2$-production rates measured for the two bisporphyrins with DPBF in methanol. This observation can be under-

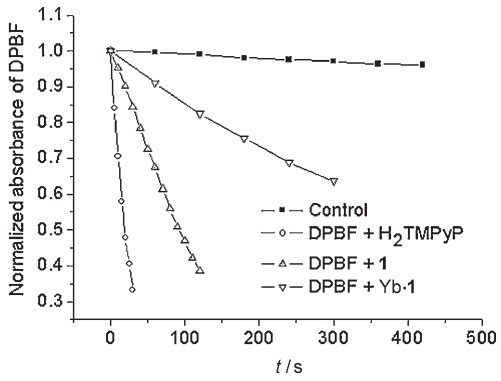

Figure 2. Normalized absorbance of DPBF (50 μM in methanol) at 415 nm as a function of time during the photoirradiation of absorbance-matched H_2TMPyP (2 μM), **1** (1 μM), and Yb·**1** (1 μM). The wavelength and power of the irradiation light source were > 500 nm and 50 W, respectively.

stood as follows: It is well established that H_2TMPyP binds to DNA;[3] therefore, both **1** and Yb·**1**, which contain the cationic TMPyP moiety, are expected to bind to DNA as well. The $^1O_2$ produced by these DNA-bound bisporphyrins upon photoirradiation can cause DNA scission very efficiently because of their proximity to the DNA target site. Therefore, a lower $^1O_2$ yield is required for observable scission than is required with an unbound photosensitizer. If Yb·**1** binds to the same DNA binding sites as **1**, it is quite possible that Yb·**1** can cause a similar degree of DNA cleavage as **1**, provided that its $^1O_2$ yield is higher than the required threshold. This notion is supported by the observation that **1** and Yb·**1** behaved similarly when their DNA-photocleavage activities were quenched by L-histidine, an $^1O_2$-selective scavenger (Figures S4C and S4D). Furthermore, no quenching of their DNA-photocleavage activities was observed when mannitol, a hydroxyl-radical scavenger, was added (data not shown). These results suggest that the amphiphilic bisporphyrins **1** and Yb·**1** are promising photodynamic therapeutic agents.

The uptake of a photosensitizer by tumor cells is a critical determinant in treatment efficacy and tumor imaging. A small molecular size and high hydrophobicity have been shown to aid the cellular uptake of a photosensitizer.[15] However, highly hydrophobic molecules may have a long retention time on the plasma membrane and a lower singlet-oxygen yield as a result of self-aggregation.[16] An appropriate balance between hydrophilicity and lipophilicity, as found in amphiphilic molecules, is therefore critical for achieving adequate tumor uptakes and treatment efficacy. Most porphyrin-based PDT agents have distinct hydrophobic and hydrophilic ends for an appropriate hydrophobicity/hydrophilicity balance. Detty and co-workers reported that a porphyrin with two carboxylic acid groups showed greater cellular uptake and antitumor efficacy than porphyrins with one, three, or four carboxylic acid functionalities.[17] Thus, the enormous flexibility in the structure of bisporphyrins, which have two porphyrin moieties with a large diversity of possible substituent combinations, should enable the generation of any required hydrophobicity/hydrophilicity balance for cellular uptake and other desired features.

The cellular uptake of H_2TMPyP, **1**, and Yb·**1** by Sarcoma 180 cells was studied by flow cytometry. The results clearly indicated that **1** was taken up rapidly by the Sarcoma 180 cells (Figure S5). After incubation for 3 h, the fluorescence intensities of the Sarcoma cells treated with **1** and Yb·**1** were at least ten times higher than those of the cells treated with H_2TMPyP. The level of fluorescence intensity of the Yb·**1**-treated cells after 22 h was very similar to that of the cells treated with **1** for the same time period. A time-dependent uptake of Yb·**1** by the Sarcoma 180 cells was also observed, and was corroborated in a quantitative fashion by the UV/Vis absorption of the cells after treatment for 22 h with the bisporphyrins (Figure 3).

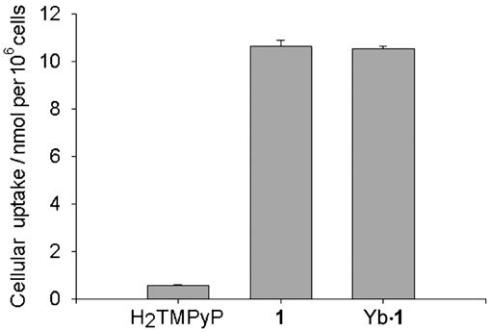

Figure 3. Spectrophotometric analysis of the cellular uptake of H_2TMPyP, **1**, and Yb·**1**. After incubation with H_2TMPyP, **1**, and Yb·**1** for 22 h, the Sarcoma 180 cells were washed thoroughly, resuspended in PBS, and then diluted to a cell density of 3.3×10^5 cells per mL. The visible-absorption spectra of these treated cell suspensions were measured spectrophotometrically (Figure S6). The amounts of the different porphyrins taken up by these cells were estimated from the measured absorbances by using calibration curves derived from the spectra of standard solutions prepared by dissolving the respective compounds in water. These uptake amounts were then divided by the cell density to afford the cellular uptake (in nmol/10^6 cells) for H_2TMPyP, **1**, and Yb·**1**.

Confocal microscopy was used to further examine the subcellular localization of H_2TMPyP, **1**, and Yb·**1** in the Sarcoma 180 cells. Figure 4 shows the confocal images of cells costained with these photosensitizers and two organelle probes specific for lysosomes and mitochondria. The localization of **1** and Yb·**1** is shown in red, and the localization of the organelle probe is shown in green. Yellow dots represent the combined confocal images of both the photosensitizer and the organelle-specific probe. Colocalization was confirmed further by analyzing the fluorescence-intensity profile drawn across the cell, as shown in the confocal micrographs. Both **1** and Yb·**1** were found to colocalize with the lysosome probe in the cytoplasm (Figure 4A and C). Significant colocalization with the mitochondria probe was not observed (Figure 4B and D). Furthermore, localization of **1** and Yb·**1** in the nucleus was not observed.

As the cellular uptake of the tetracationic porphyrin H_2TMPyP was many times lower than that of the amphiphilic bisporphyrins **1** and Yb·**1** (Figure 3), we were unable to obtain a high-resolution confocal image of the subcellular localization of H_2TMPyP. To capture the weak fluorescence signals from the H_2TMPyP-treated cells, we increased the pinhole size of the

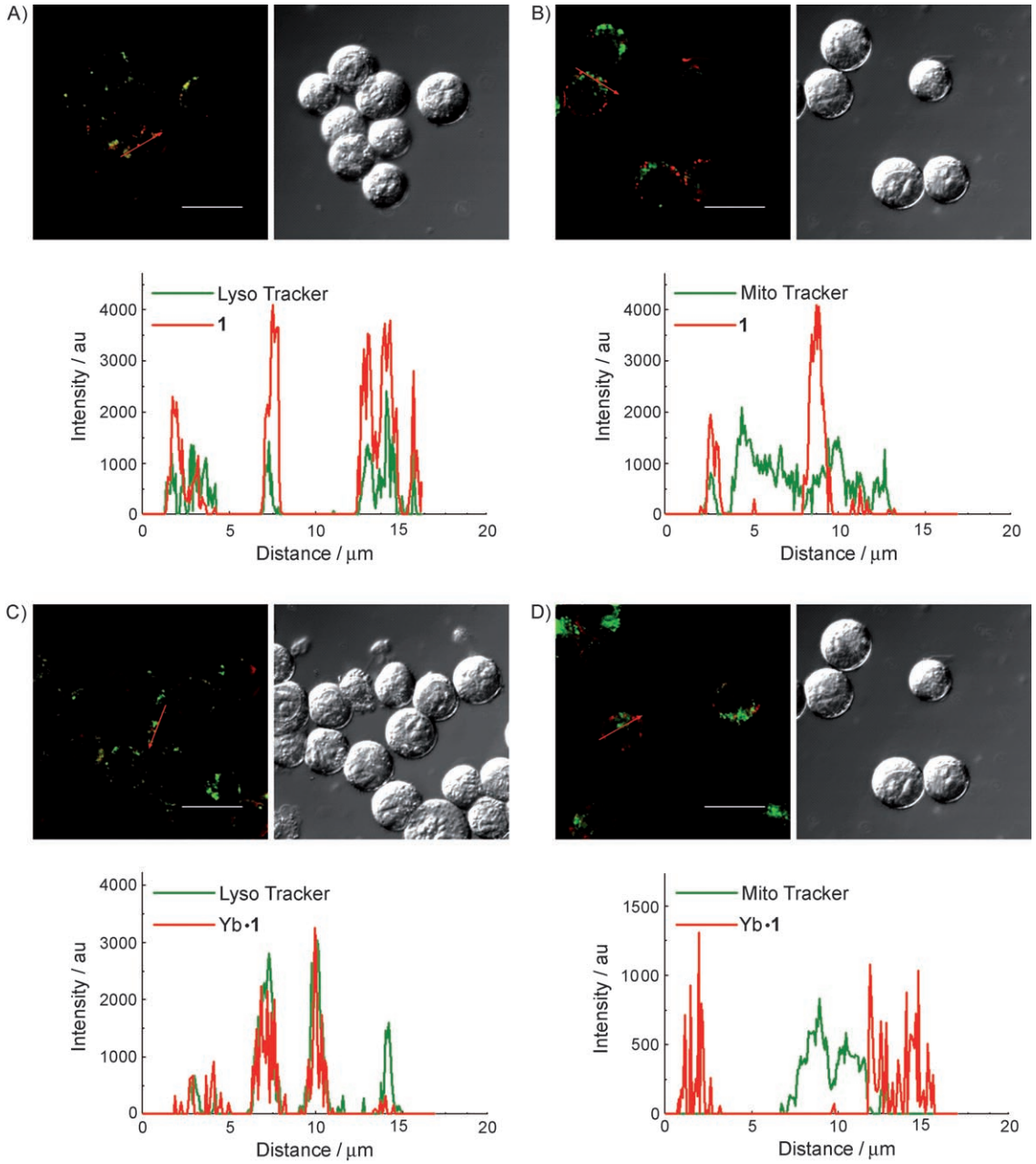

Figure 4. Confocal images of Sarcoma 180 cells treated with **1** [A) LysoTracker, B) MitoTracker] or Yb·**1** [C) LysoTracker, D) MitoTracker]. Sarcoma 180 cells were incubated with **1** or Yb·**1** (4 μM) for 22 h. The cells were then stained with the mitochondria probe MitoTracker Green FM dye M7514 (300 nM) or the lysosome probe LysoTracker Green DND-26L7526 (70 nM) for 30 min. Upper panel: Confocal (left) and bright-field (right) images. Red dots represent the fluorescence from **1** (or Yb·**1**), and green dots represent the fluorescence from the organelle probes. Yellow dots represent the overlapping fluorescent signals from **1** (or Yb·**1**) and the organelle probes. Lower panel: Fluorescence-intensity profiles of **1** (or Yb·**1**) and the organelle probes along the red arrow shown in the confocal micrographs. Scale bar: 20 μm.

confocal microscope to 500 μm (see the fluorescence images in Figure S7 A and B). Only a small amount of H_2TMPyP was observed in the cytoplasm, and apparent colocalization of H_2TMPyP and the organelle probes was not observed.

To examine the therapeutic usefulness of these systems, the photocytotoxicity of H_2TMPyP, **1**, and Yb·**1** towards Sarcoma 180 cells was measured by a MTT-reduction assay (Figure 5; MTT = 3-(4,5-dimethylthiazol-2-yl)-2,5-diphenyltetrazolium bromide). The bisporphyrin **1** is more efficacious in PDT than Yb·**1** or H_2TMPyP. At a concentration of 4 μM, the light dose required for **1**, Yb·**1**, and H_2TMPyP to kill 50% of the Sarcoma cells (LC_{50}) was approximately 3, 6.2, and 14 J cm^{-2}, respectively. Although H_2TMPyP exhibits a higher $^1O_2$ yield than **1** and Yb·**1**, its photocytotoxicity was substantially lower than that of **1** and Yb·**1**, probably as a result of its poor cellular uptake (Figure 3). The level of cellular uptake of **1** and Yb·**1** is similar; the higher photocytotoxicity of **1** relative to that of Yb·**1** is probably due to the higher $^1O_2$ yield of **1** (Figure 2).

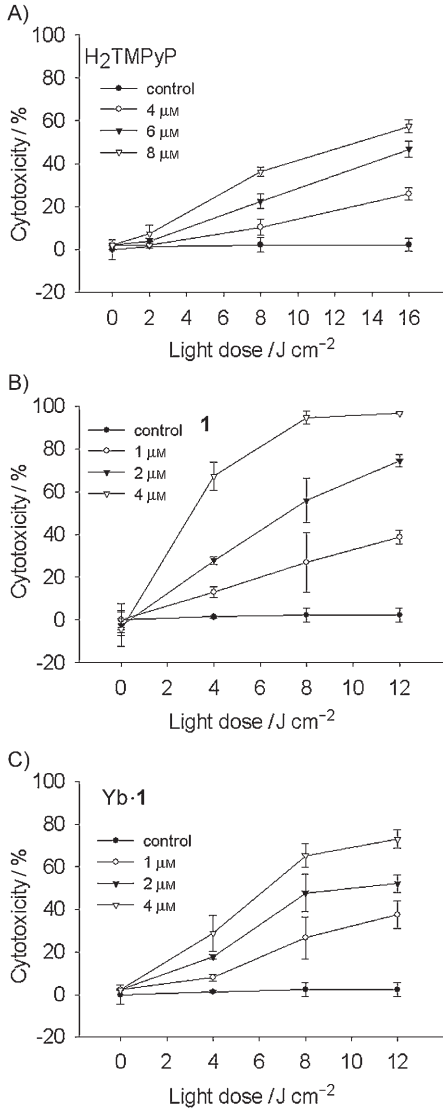

Figure 5. Photocytotoxicity of A) H_2TMPyP, B) **1**, and C) Yb·**1** towards Sarcoma 180 cells. The cells were treated with the drugs at various concentrations for 22 h, then washed with fresh medium, and irradiated with various doses of light. The MTT cytotoxicity assay was carried out 22 h after PDT. The results are expressed as the mean ± S.D. of four experiments.

Apoptosis and necrosis are two major forms of cell death. They can be differentiated on the basis of their characteristic morphological features.[18] In this study, flow cytometry and fluorescence microscopy were used to analyze the mode of cell death after PDT. Neither a sub-G1 peak (Figure S8) nor apoptotic nuclei (Figure S9) were observed in the cells after PDT with **1**. The pattern of nuclear staining of Sarcoma 180 cells subjected to PDT with Yb·**1** was similar to that observed for cells subjected to PDT with **1** (data not shown). The subcellular localization of **1** and Yb·**1** in lysosomes (Figure 4A and C) and the subsequent photodamage of lysosomes with the release of lysosomal enzymes into the cytoplasm might explain the induction of necrosis of the Sarcoma 180 cells.

The PDT efficacy of a photosensitizer varies for different cell lines but depends largely on the hydrophobicity and hydrophilicity of the photosensitizer. Greater hydrophobicity leads to higher cellular uptake but also to a lower yield of singlet oxygen as a result of self-aggregation. Conversely, increased hydrophilicity results in an increased yield of singlet oxygen but lower cellular uptake. This generalization was found to be true for the systems investigated in this study, and amphiphilic photosensitizers are generally more active photodynamically than hydrophobic and hydrophilic molecules of the same structural class.[19] Moreover, amphiphilic photosensitizers are pharmacokinetically favorable for rapid systemic clearance and tumor selectivity.[20] It was reported previously that the tumor selectivity of amphiphilic photosensitizers is related to their more efficient binding to low-density lipoproteins in the transport of porphyrins to tumor tissues.[21] Furthermore, high-molecular-weight porphyrins accumulate preferentially in solid tumors, and relatively large porphyrins are expected to be internalized in membrane-bound organelles; thus, their localization in the intracellular compartment occurs in a controlled manner.[22] However, there have been few studies on the photodynamic properties of bisporphyrins.[23] Herein, we presented a method of synthesizing an amphiphilic bisporphyrin with an appropriate hydrophobicity/hydrophilicity balance through a convenient modification of H_2TMPyP. The amphiphilic bisporphyrins **1** and Yb·**1** exhibited a tenfold higher cellular uptake by Sarcoma 180 cells relative to H_2TMPyP. More importantly, the NIR-luminescence properties of Yb·**1** make it a suitable compound for tumor imaging and use as a PDT agent in the "see and treat" approach, which enables optimal therapeutic efficacy. A study of the imaging and therapeutic applications of such bisporphyrins is under way.

Acknowledgement

We thank Dr. H. L. Tam and Y. M. Lee for their excellent technical help. We also thank the Hong Kong Baptist University (Grant FRG/03-04/II-05), the Hong Kong Research Grants Council (Grant HKBU 2023/04P), and the National Natural Science Foundation of China (Grant No. 30570015, 20621502) for financial support.

Keywords: amphiphiles · photodynamic therapeutics · porphyrinoids · tumor imaging · ytterbium

[1] T. Hasan, B. Ortel, A. C. E. Moor, B. W. Pogue in *Holland-Frei Cancer Medicine 6* (Eds.: D. W. Kufe, R. E. Pollock, R. R. Weichselbaum, R. C. Bast, Jr., T. S. Gansler, J. F. Holland, E. Frei III), Decker, Hamilton, **2003**, pp. 605–622.

[2] D. E. J. G. J. Dolmans, D. Fukumura, R. K. Jain, *Nat. Rev. Cancer* **2003**, *3*, 380–387.

[3] a) H. Mita, T. Ohyama, Y. Tanaka, Y. Yamamoto, *Biochemistry* **2006**, *45*, 6765–6772; b) K. E. Thomas, D. R. McMillin, *J. Phys. Chem. B* **2001**, *105*, 12628–12633; c) I. Haq, J. O. Trent, B. Z. Chowdhry, T. C. Jenkins, *J. Am. Chem. Soc.* **1999**, *121*, 1768–1779; d) R. T. Wheelhouse, D. Sun, H. Han, F. X. Han, L. H. Hurley, *J. Am. Chem. Soc.* **1998**, *120*, 3261–3262; e) R. F. Pasternack, R. A. Brigandi, M. J. Abrams, A. P. Williams, E. J. Gibbs, *Inorg. Chem.* **1990**, *29*, 4483–4486.

[4] a) J. Nuno Silva, J. Haigle, J. P. C. Tomé, M. G. P. M. S. Neves, A. C. Tomé, C. Mazière, R. Santus, J. A. S. Cavaleiro, P. Filipe, P. Morlière, *Photochem. Photobiol. Sci.* **2006**, *5*, 126–133; b) L. Chaloin, P. Bigey, C. Loup, M. Marin, N. Galeotti, M. Piechaczyk, F. Heitz, B. Meunier, *Bioconjugate*

Chem. **2001**, *12*, 691–700; c) M. B. Vrouenraets, G. W. M. Visser, C. Loup, B. Meunier, M. Stigter, H. Oppelaar, F. A. Stewart, G. B. Snow, G. A. M. S. van Dongen, *Int. J. Cancer* **2000**, *88*, 108–114.

[5] a) G. Li, A. Slansky, M. P. Dobhal, L. N. Goswami, A. Graham, Y. Chen, P. Kanter, R. A. Alberico, J. Spernyak, J. Morgan, R. Mazurchuk, A. Oseroff, Z. Grossman, R. K. Pandey, *Bioconjugate Chem.* **2005**, *16*, 32–42; b) S. K. Pandey, A. L. Gryshuk, M. Sajjad, X. Zheng, Y. Chen, M. M. Abouzeid, J. Morgan, I. Charamisinau, H. A. Nabi, A. Oseroff, R. K. Pandey, *J. Med. Chem.* **2005**, *48*, 6286–6295; c) Y. Chen, A. Gryshuk, S. Achilefu, T. Ohulchansky, W. Potter, T. Zhong, J. Morgan, B. Chance, P. N. Prasad, B. W. Henderson, A. Oseroff, R. K. Pandey, *Bioconjugate Chem.* **2005**, *16*, 1264–1274; d) J. L. Sessler, N. A. Tvermoes, J. Davis, P. Anzenbacher, Jr., K. Jursikova, W. Sato, D. Seidl, V. Lynch, C. Black, A. Try, B. Andrioletti, G. Hemmi, T. D. Mody, D. Magda, V. Kral, *Pure Appl. Chem.* **1999**, *71*, 2009–2018.

[6] a) A. Zaheer, T. E. Wheat, J. V. Frangioni, *Mol. Imaging* **2002**, *1*, 354–364; b) Y. Lin, R. Weissleder, C.-H. Tung, *Bioconjugate Chem.* **2002**, *13*, 605–610.

[7] a) R. Weissleder, V. Ntziachristos, *Nat. Med.* **2003**, *9*, 123–128; b) J. V. Frangioni, *Curr. Opin. Chem. Biol.* **2003**, *7*, 626–634; c) E. M. Sevick-Muraca, J. P. Houston, M. Gurfinkel, *Curr. Opin. Chem. Biol.* **2002**, *6*, 642–650.

[8] P. Rolfe, F. Scopesi, G. Serra, *Measurement Sci. Technol.* **2007**, *18*, 1683–1688.

[9] M. I. Gaiduck, V. V. Grigoriants, A. F. Mironov, L. D. Roitman, V. I. Chissov, V. D. Rumiantseva, G. M. Sukhin, *Dokl. Akad. Nauk SSSR* **1989**, *308*, 980–983.

[10] a) J.-C. G. Bünzli, S. Comby, A.-S. Chauvin, C. D. B. Vandevyver, *J. Rare Earths* **2007**, *25*, 257–274; b) J.-C. G. Bunzli, *Met. Ions Biol. Syst.* **2004**, *42*, 39–75.

[11] a) W. K. Wong, X.-J. Zhu, W. Y. Wong, *Coord. Chem. Rev.* **2007**, *251*, 2386–2399, and references therein; b) W. K. Wong, A. Hou, J. Guo, H.-S. He, L.-L. Zhang, W. Y. Wong, K. F. Li, K. W. Cheah, F. Xue, T. C. W. Mak, *J. Chem. Soc. Dalton Trans.* **2001**, 3092–3098.

[12] We also measured the NIR-luminescence spectrum of Yb·**1** upon photoirradiation at 523 nm. At this wavelength, TMPyP absorbed much more intensely than Yb·**1**, and therefore only the TMPyP moiety was photoexcited. However, because of the much weaker laser light source used for this excitation wavelength (a Nd:YAG (neodymium-doped yttrium aluminum garnet) optically pumped oscillator (OPO) pulsed laser), the signal-to-noise ratio of the emission spectrum was not as good as that of the emission spectrum obtained by using an argon-ion laser ($\lambda_{ex}=$ 514 nm; Figure 1). We also observed energy transfer of this type during our previous study of a series of heterodimetallic bisporphyrins: F.-L. Jiang, W.-K. Wong, X.-J. Zhu, G.-J. Zhou, W.-Y. Wong, P.-L. Wu, H.-L. Tam, K.-W. Cheah, C. Ye, Y. Liu, *Eur. J. Inorg. Chem.* **2007**, 3365–3374. We then found that the photoexcitation of different metalloporphyrin moieties resulted in different intensities of NIR emission from the L_{OMe}^--capped Yb^{III}–porphyrins with the following trend: Pt^{II}–$Yb^{III} > Pd^{II}$–$Yb^{III} > Zn^{II}$–Yb^{III}.

[13] A. Beeby, I. M. Clarkson, R. S. Dickins, S. Faulkner, D. Parker, L. Royle, A. S. de Sousa, J. A. G. Williams, M. Woods, *J. Chem. Soc. Perkin Trans. 2* **1999**, 493–503.

[14] K. Oda, S. Ogura, I. Okura, *J. Photochem. Photobiol. B* **2000**, *59*, 20–25.

[15] C. A. Puckett, J. K. Barton, *J. Am. Chem. Soc.* **2007**, *129*, 46–47.

[16] G. N. Georgiou, M. T. Ahmet, A. Houlton, J. Silver, R. J. Cherry, *Photochem. Photobiol.* **1994**, *59*, 419–422.

[17] Y. You, S. L. Gibson, R. Hilf, S. R. Davies, A. R. Oseroff, I. Roy, T. Y. Ohulchanskyy, E. J. Bergey, M. R. Detty, *J. Med. Chem.* **2003**, *46*, 3734–3747.

[18] W. N. Leung, X. Sun, N. K. Mak, C. M. N. Yow, *Photochem. Photobiol.* **2002**, *75*, 406–411, and references therein.

[19] a) N. Cauchon, H. Tian, R. Langlois, C. L. Madeleine, S. Martin, H. Ali, D. Hunting, J. E. van Lier, *Bioconjugate Chem.* **2005**, *16*, 80–89; b) P. Margaron, M. J. Grégoire, V. Scasnar, J. E. van Lier, *Photochem. Photobiol.* **1996**, *63*, 217–223.

[20] R. Bonnett, *Rev. Contemp. Pharmacother.* **1999**, *10*, 1–17.

[21] D. Kessel, P. Thompson, K. Saito, K. D. Nantwi, *Photochem. Photobiol.* **1987**, *45*, 787–790.

[22] N. Nishiyama, H. R. Stapert, G.-D. Zhang, D. Takasu, D.-J. Jiang, T. Nagano, T. Aida, K. Kataoka, *Bioconjugate Chem.* **2003**, *14*, 58–66.

[23] R. K. Pandey, K. M. Smith, T. J. Dougherty, *J. Med. Chem.* **1990**, *33*, 2032–2038.

Received: December 19, 2007
Published online on March 26, 2008

